Quantification of Corona Discharges on Nonceramic Insulators

B. Pinnangudi, R. S. Gorur and A. J. Kroese [*]
Department of Electrical Engineering, Arizona State University, Tempe, AZ
[*] Salt River Project, Phoenix, AZ

Abstract: This paper attempts to establish a correlation of the visual images of corona obtained from a camera with discharge magnitude measured with conventional partial discharge equipment. A linear relationship is shown between the transformed image parameters and the discharge magnitude, thereby providing a means for quantifying corona observations made during routine maintenance inspections of insulators from ground. Different insulator designs using silicone rubber (SIR) and ethylene propylene diamene monomer (EPDM) housings were examined. The effect of fog has been examined by performing experiments inside a fog chamber. It is shown that this information can be used along with the corona degradation characteristics of housing materials to identify discharge patterns that can pose problems to the integrity of the insulator.

Index terms:
Insulators, hydrophobicity, partial discharge, corona, field inspection, image processing.

Introduction:

Corona discharges can be a significant threat to the integrity of nonceramic insulators (NCI) due to the organic nature of the housing material [1]. For transmission class insulators (69 kV and above), corona can be problem not only in contaminated but in clean environments as well. From worldwide experience it has been identified that a majority of NCI applications are under relatively clean or lightly contaminated conditions. On NCI, corona can be present locally for long periods of time due to inadequate hardware design, damaged hardware, deficient interfaces due to improper design and/or manufacturing. Field inspections on 230 kV and 500 kV insulators confirm the existence of corona even under relatively dry and clean conditions [2].

In practical high-voltage systems it is difficult to avoid corona in the field, especially under wet and contaminated conditions [3, 4]. Hence, knowledge of the corona discharge magnitude and damage threshold of the housing material is essential. Corona is responsible for multiple effects such as mechanical, due to the impingement of charged particles, ultraviolet (UV) radiation, and liberation of ozone. Highly oxidizing and hydrated species of nitrogen oxides are generated which on dissolving in moisture leads to the formation of acids [5, 6]. Fig. 1 shows two pictures of the damage caused by corona on NCI during service. Fig. 1(a) is obviously an advanced stage of degradation while Fig. 1(b) shows degradation that could still be considered minor. Any cracks in the housing can expose the fiberglass core to moisture. The exposed rod can fail by tracking, erosion or brittle fracture [7, 8, 9], leading to premature failure. Hence, there is a necessity to periodically inspect NCI and replace degraded insulators in a timely manner.

The methods currently used by the utilities to inspect in-service NCI are,

- Acoustic emission,
- Radio interference voltage (RIV) measurement,
- Infra-red (IR) thermography,
- Electric-field measurement,
- Visual observation,
- Daytime corona detection with UV camera.

Both, acoustic emission and radio interference voltage measurement methods are sensitive to background noise. They cannot be used to determine the precise location of the discharge on the insulator. It is a significant drawback as discharges on insulator hardware cannot always be avoided and may not need immediate replacement, while discharges on housing can be a harbinger to serious problems in future.

Determination of surface temperature by IR thermography has yielded partial success. However, this method but cannot be used to detect small defects are incapable of causing a significant change in the surface temperature. The reliability of IR thermography is also reduced when performed under hot and sunny conditions [10]. Electric field measurement along the

insulator has been more successfully employed for ceramic than nonceramic insulators due to inherent differences in the construction of these insulators. Also it has been shown that the method can yield erroneous results in the presence of moisture [10]. Besides, this method requires deployment from the tower or bucket truck and hence is not convenient.

For all the above reasons visual observation by knowledgeable personnel either from ground or helicopters still remains the most effective method for NCI inspection. Special UV cameras to detect corona in daytime are increasingly being used by the utilities for periodic inspections. These cameras can provide information on the exact location of corona. Due to the high sensitivity of these cameras, it is common that corona is seen on insulators quite frequently. But because there is no information on the magnitude of the discharge it is difficult to base any decisions on insulator maintenance or replacement on just visual observations. This paper attempts to quantify these corona images with the hope that this would provide a better basis for taking corrective actions.

There are essentially two different manufacturers of corona cameras at the present time. The experiments and field inspections reported in this paper correspond to two different models from the same manufacturer (COROCAM 2 and COROCAM 3 [11]). While future generations of such cameras will undoubtedly incorporate a number of refinements, it is expected that the procedure described in this paper for establishing the correlation between the visual images and discharge magnitude will still be applicable.

Principle of Operation of Corona Camera

Visual observation of corona with the unaided eye is difficult because corona emits weak radiation, mostly in the ultra-violet (UV) spectral range, and is therefore invisible. A typical spectral distribution of corona from a point-plane electrode configuration is shown in Fig. 2. The experiment was performed in the laboratory using a Raman spectrometer (Acton SP-275, 1200 g/mm grating, Princeton charge coupled detector (CCD), 8 cm^{-1}/pixel resolution). The corona source was a high voltage needle at a distance of 5 cm from the plane electrode. The entire arrangement was 1 m away from the CCD.

It can be seen from Fig. 2 that corona discharges in air emit light mainly in the 230 - 405 nm range. The most intense emissions are around 300 - 360 nm. The solar radiation in the 300 - 360 nm region is much stronger than the corona thus masking the corona signals. In the "solar-blind" region (240-280 nm), the corona emission is much weaker. However, the solar background is negligible. It is these signals generated by corona in the solar-blind region that are used by the cameras to detect corona.

The camera detects weak corona signals by overlaying a UV video image of the corona on a visible video image of the background. The solar blindness is achieved by using a special filter that is transparent in the solar blind UV band and is completely opaque to the solar radiation. A sophisticated lens and filter system is used to project the UV light emitted by corona discharges onto an optoelectric device, which is then amplified and transferred to a CCD detector that generates the image.

A special filter that transmits light between 240-280 nm and completely blocks longer wavelengths is combined with photon-counting intensified charge coupled devices (CCD) so that it responds only to the corona emission spectrum corresponding to the solar blind region. The optical spectrum transmits the same scene to the visible-light camera enabling it to present a view of the source of discharge in perfect registration, without parallax.

Image analysis and processing

The image captured is stored in a computer as a matrix of pixels in a JPG file. This image requires a number of processing and noise removal steps to facilitate mathematical operations and quantitative analysis [12]. The JPG file represents the light intensity levels at different locations of the image matrix. A 240 x 640 image matrix was used for the purposes of the present study. The image matrix dimensions can be selected by changing the resolution settings.

The captured images are associated with inaccuracies caused by spurious light signals from the background and microscopic dust particles surrounding the sample. This image needs to be processed to render it free of noise. The flowchart for image processing of corona image is illustrated in Fig. 3.

By using a MATLAB program, the pixel intensities (represented by the elements of the image matrix) are summed up to obtain the cumulative intensity [13]. The maximum pixel intensity level (I_m) of the background image is determined. In the output corona image, pixels that have intensities higher than I_m are considered illuminated (pixels that have intensities higher than I_m are considered '1' or high, and otherwise '0' or low). The number of illuminated pixels is a measure of the illuminated pixel area. The cumulative intensity and the illuminated pixel area are referred to as transformed image parameters in the subsequent sections of the paper.

Corona pixel identification and filtering is achieved by determining the places in the corona image where there is an abrupt change in the intensity level, using either one of the criteria suggested below,

- The first derivative of the intensity is larger in magnitude than some predefined threshold,
- The second derivative of the intensity has a zero crossing.

To improve the accuracy of the technique, two different thresholds are used; one to detect pixels corresponding to region of strong discharges and the other to detect pixels corresponding to regions of weak discharges. The weak corona pixels should typically be connected to strong corona pixels to be accounted for as an illuminated corona pixel [14]. Hence the suggested technique is less sensitive to noise unlike traditional PD techniques and can effectively identify weak corona pixels. Two methods were adopted to distinguish the corona from the noise pixels:

(i) Background subtraction technique

Two images are captured, one of which is of the region of discharge while the other is the image of a region close to the region of discharge. On subtracting the individual pixel intensities of the two images, the spurious light signals are cancelled. The retained pixel intensities are only that of the corona discharges.

(ii) Background analysis technique

Both the accuracy and robustness of the method are improved by observing the background image and the corona image at the same location of interest on the insulator. I_m is determined from the captured background image. Here, the background image implies the image

of the insulator with no corona. In the final image (corona+background), the pixels with intensity magnitudes less than I_m are filtered out.

As the noise level approaches the corona intensity it is more difficult to filter out the noise. Hence it is suggested to avoid exposing the camera to bright light while measurement. The lesser the ambient light, the more effective and accurate is the suggested technique.

Parameter Extraction

1) Radial Extent, R

   This is calculated by finding the light emission pixel (x_i, y_i) in the processed image array that is farthest from the center of discharge (x_c, y_c)

   $$R = \sqrt{(x_i - x_c)^2 + (y_i - y_c)^2}$$

2) Area Growth, A

   The area is calculated by calculating all the pixels that are part of the corona discharge or light emission spectrum. The area is therefore obtained by multiplying the area of a single pixel with the number of illuminated pixels.

3) Light Intensity, I

   Light intensity is calculated by performing a weighted sum of all the pixels that are part of the light emission spectrum. The pixel intensity is measured relative to the base noise level.

   $$I = \sum_{n=1}^{N} I_{pixel} - I_{base}$$

Where N is the number of pixels in the region of interest [15].

Experimental Setup:

The experimental setup used in the present study is illustrated in Fig. 4. The high-frequency corona pulses are picked up by the coupling quadripole (CQ) and routed to the detector (HAEFELY partial discharge detector type 561, sensitivity 1 pC). The detector can be

used either in the straightforward method or in a bridge circuit. The apparent charge is measured in the detector by quasi-integration in pre-selectable frequency ranges.

A 115 kV rated silicone rubber insulator and an EPDM insulator removed from the field were chosen for the initial experiments. The silicone rubber and the EPDM insulator designs are shown schematically in Fig. 5a and Fig. 5b respectively. The silicone rubber insulator chosen for the experiment had an unusually rough line end fitting. The hardware also displayed burn marks caused by lightning events. The voltage applied was increased gradually to the rated voltage in steps of 5 kV. The corona images and their corresponding PD magnitudes were recorded simultaneously. For convenience, the distance between the point of interest and the camera was selected to be $5\,m$.

Any increase in the voltage from the inception value resulted in higher discharge magnitudes (measured by PD detector), as shown in Fig. 6 and Fig. 7. By using the proposed technique the intensity plots were constructed and cumulative intensities were determined. The cumulative intensity values were approximately zero and 150 arbitrary units in the transformed parameter scale corresponding to 30 pC and 2 nC discharge magnitudes respectively. The increase in discharge magnitude is manifested as an increase in the transformed parameter values [16, 17, 18]. It is interesting to note that corona was observed even below the normal operating voltage, and this is attributed to the hardware that was weathered during field use.

Results and Discussions

By changing the voltage in steps of 5 kV, the corona discharge magnitude was varied and the corresponding transformed parameter values were determined. Figs. 8 and 9 show the results of the transformed parameters as a function of the PD discharge magnitudes. The discharge magnitude associated with corona can be seen to be proportional to the intensity of the luminous discharge and the discharge area.

To study the effects of the housing material on the suggested technique, the above experiments were replicated on an EPDM insulator whose design is shown schematically in Fig. 5b. Figs. 10 and 11 are corona images and their corresponding intensity plots for this EPDM insulator. The cumulative intensities were found to be 12 and 140 units in the transformed parameter scale. The discharge magnitudes corresponding to the transformed parameter values

were found to be 0.1 nC and 1.85 nC by using Figs. 8 and 9. The PD measurements corresponding to corona observed in Figs. 10 and 11 with the PD detector were 0.2 nC and 1.9 nC. The calculated values from the proposed technique hence matched well with the discharge magnitudes measured by the PD detector. It is interesting to note the occurrence of corona at the interface between the individually jointed sheds under wet conditions even for a new insulator. Fig. 12 is a three dimensional representation of the plot shown in Fig. 11b, from which it is easier to visualize the location of corona discharge on the insulator.

There are several regions in a non-ceramic insulator that serve as preferential locations for corona discharges. These are:

- The hardware of the insulator even under dry conditions in the absence of a grading ring, as shown in Fig. 13a.
- The hardware and the hydrophobic housing material, especially in the presence of water droplets. This is shown in Figs. 13b and 13c
- Interfaces created by joining individual sheds (Fig. 5) especially in the presence of water droplets. This is shown in Fig. 13d.
- The shank portion between high voltage end fitting and first shed especially under wet conditions, as shown in Fig. 13e.

The cumulative intensities were calculated by the proposed method for each the corona images depicted in Fig. 13. The cumulative intensity and area plot for the different images is shown in Fig. 14. The discharge magnitudes corresponding to these cumulative intensities matched closely the PD magnitudes indicated by the PD detector.

Knowledge of the discharge location is important. Discharges that occur on the hardware and/or far from the housing material are less damaging when compared to discharges that occur on or in close proximity to the housing. The ratio of the cumulative intensity to the area of the illuminated pixels is a measure of the corona discharge density and could be a good predictor of degradation. On visual observation of Fig. 13 and from Figs. 14a and 14b, it might appear that the corona corresponding to Figs. 13d and 13e have no significant damaging effect when

compared to the corona corresponding to the image in Fig. 13a. However, Fig. 14c indicates otherwise.

Effect of distance

The pixel intensities and illuminated pixel area in the corona image were found to diminish with increasing distance between the camera and the insulator under observation for the same magnitude of discharge. To account for the distance factor, the insulator was subjected to a constant discharge magnitude and the discharge image was captured at different distances of the camera from the point of interest. Due to the size of the laboratory a correlation was established between the transformed image parameters and distance up to about $10\,m$. The curve is extrapolated to determine the correlation between the transformed image parameters and distances beyond $10\,m$. The equation of the fitted curve for the data points up to $10\,m$ was used for extrapolation up to $50\,m$. Fig. 15 shows the plot of pixel intensity as a function of distance for different PD magnitudes. It can be seen that as we move farther away from the insulator the discharge magnitude threshold for detection increases.

Effect of Fog

Field inspections of corona can be hampered by foggy conditions. Due to scattering and absorption of light a reduced percentage of the transmitted light reaches the receiver under foggy conditions. All data reported in this paper thus far pertain to observations in an air-conditioned laboratory which has a 40% relative humidity level. The effect of fog was studied by subjecting the insulator to varying levels of fog inside an enclosed chamber. The fog density was characterized in terms of the relative humidity within the chamber.

For the same discharge magnitude, the number of illuminated pixels and hence the corresponding cumulative pixel intensity and illuminated pixel area were reduced with increasing fog density. Depending on the fog density, there is a discharge magnitude below which corona cannot be observed. Below the cut-off point a linear relationship is obtained between the pixel intensity (and pixel area) and discharge magnitude, as shown in Fig. 16.

Application to Field Inspections

Figs. 17 and 18 show images of corona obtained from field inspection performed twilight conditions in October when the relative humidity was about 40%. The distance between the

corona camera and the region of discharge was estimated to be 50 meters. Fig. 17 represents corona on a 230 kV first generation EPDM insulator design with individually jointed sheds (Fig. 5b), used in earlier experiments for this paper. This insulator was installed more than 20 years back without corona rings, as the need for corona rings was not discovered at that time. Fig. 18 shows a 500 kV line post insulator used as a jumper in a substation. The presence of the bundled conductor and the large size of the line end hardware were thought to provide adequate electric stress grading, hence no additional rings were installed. The corresponding processed image and intensity plots are also shown in these figures.

The cumulative intensity was determined to be 55 and 37 (Arbitrary Units) for Figs. 17 and 18 respectively. The corona discharges seen in Fig. 17 can be more harmful than the discharges observed in Fig. 18 due to its proximity to the housing material and the effective magnitude of discharges that terminate on the shed. From Figs 15 and 16, it is determined that the images corresponded to partial discharge magnitudes of 3 nC and 2 nC respectively.

Knowing the corona discharge magnitude is part of the problem. The other part is to determine the corona degradation characteristics of different housing materials. In a recent paper this aspect was explored and the time for manifestation of damage from corona was determined for several NCI housing materials [19]. Since this aspect is dependent on the formulation it is important to have this data in order to determine if the observed corona during field inspection is harmful to the insulator.

Users need to create a database listing the discharge magnitude (or density) for every inspection. This will help establish if there are particular designs and field locations where corona can be more problematic than for others. Appropriate maintenance can therefore be performed in a timely manner.

Conclusions

1) The images provided by the corona-sensitive camera can be translated into quantifiable parameters.

2) There is good correlation between the visual image and the corona discharge magnitude.

3) The effect of distance and foggy conditions on the visual image have been investigated

4) The results obtained have been applied to field inspection of NCI.

References

[1] V. M. Moreno and R. S. Gorur, "Effect of long-term corona on non-ceramic outdoor insulator housing materials," IEEE Trans. on Dielectrics and Electrical Insulation, Vol. 8, No. 1, pp. 117-128, 2001.

[2] V. M. Moreno, "Effect of long-term corona on non-ceramic outdoor insulator housing material," PhD Dissertation, Arizona State University, August 2001.

[3] A. J. Phillips, R. H. Billings, and H. M. Schneider, "Water drop corona effects on full-scale 500 kV non-ceramic insulators," IEEE Trans. Power Delivery, Vol. 14, No. 1, pp. 258-265, Jan. 1999.

[4] A. J. Phillips, D. J. Childs, and H. M. Schneider, "Aging of non-ceramic insulators due to corona from water drops," IEEE Trans. Power Delivery, Vol. 14, No. 3, pp. 1081-1089, July 1999.

[5] A. A. Kulikovski, "Production of chemically active species in the air by a single positive streamer in a non-uniform Field," IEEE Trans. Plasma Science, Vol. 25, No. 3, pp. 439-446, 1997.

[6] M. M. Shahin, "Ionic reactions in corona discharges of atmospheric gases," Advances in chemistry series: Chemical Reactions in Electrical Discharges, Vol. 80, pp. 48-58, 1969.

[7] N. Yoshimura, S. Kumugai and S. Nishimura, "Electrical and environmental aging of silicone rubber used for outdoor insulation," IEEE Trans. on Dielectrics and Electrical Insulation, Vol. 6, No. 5, pp. 632-650, 1999.

[8] V. M. Moreno and R. S. Gorur, "Ac and dc performance of polymeric housing materials for HV outdoor insulators," IEEE Trans. on Dielectrics and Electrical Insulation, Vol. 5, No. 3, pp. 342-350, 1999.

[9] J. Montesinos, R. S. Gorur, B. Mobasher and D. Kingsbury, "Mechanism of brittle fracture in non ceramic insulators," IEEE Trans. Dielectrics and Electrical Insulation, Vol. 9, No. 2, pp. 236-243, April 2002.

[10] R. S. Gorur, E. Cherney and J. T. Burnham, "Outdoor insulators," Arizona, USA: Ravi S. Gorur, Inc., ISBN 0-9677611-0-7, 1999.

[11] Anonymous, "Corocam," CSIR, www.corocam.com

[12] T. Asokan and T. S. Sudarshan, "Streak photography of the dynamic-electrical discharge behavior on insulator surfaces in vacuum," IEEE Trans. on Electrical Insulation, Vo. 28, No. 1, pp. 101-110, February 1993.

[13] J. D. Cross and T. S. Sudarshan, "High speed photography of surface flashover across high density alumina in vacuum under direct and impulse voltages," IEEE Trans. on Electrical Insulation, Vo. 11, pp. 63-66, 1976.

[14] V. P. Afanas'ev, A. M. Chaly, A. A. Logatchev, S. M. Shkol'nik and K. K. Zabello, "Computer-aided reconstruction of cathode images obtained by high speed photography of high current vacuum arcs," IEEE Trans. on Plasma Science, Vo. 29, No. 5, pp. 695-699, October 2001.

[15] B. N. Pinnangudi, R. S. Gorur and A. J. Kroese, "Energy quantification of corona discharges on polymer insulators," 2002 IEEE Conf. on Electrical Insulation and Dielectric Phenomena, pp. 315-318, 2002.

[16] G. Dyogo and J. D. Cross, "Influence of injected plasma on oscillations of cathode luminosity in triggered vacuum breakdown," IEEE Trans. on Plasma Science, Vo. 21, No. 5, pp. 407-409, October 1993.

[17] T. S. Asokan and T. S. Sudarshan, "Pre-flashover luminosity along an alumina/vacuum interface," IEEE Trans. on Electrical Insulation, Vol. 1, No. 6, pp. 1180-1185, December 1994.

[18] C. R. Li and T. S. Sudarshan, "Characteristics of preflashover light emission from dielectric surfaces in vacuum," IEEE Trans. on Electrical Insulation, Vol. 2, No. 3, pp. 483-491, June 1995.

[19] V. M. Moreno, R. S. Gorur and A. J. Kroese, "Impact of corona on long-term performance of nonceramic insulators," IEEE Trans. on Dielectrics and Electrical Insulation, Vol. 10, No. 1, pp. 80-95, 2003.

	Balasubramanian Pinnangudi was born in Chennai (India) in the year 1980. He received his bachelor's degree from Madras University (India) in 2001. He holds a master's degree (Thesis: Energy Quantification of Corona Discharges on Non-ceramic Insulators) from the Electrical Engineering Department, ASU in 2003. He is currently pursuing his PhD degree and working on Life Prediction of Non-ceramic insulators. His interest is on the use of polymeric materials for outdoor application.
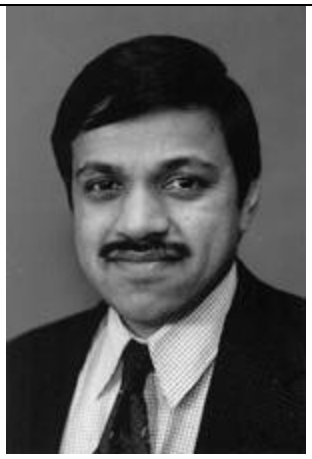	Ravi S. Gorur is a professor in the Electrical Engineering Department at Arizona State University (ASU). He is responsible for numerous research projects in the areas of insulators for electric power transmission and distribution, sponsored by utilities, government and industry. He has published a textbook on Outdoor Insulators and over 100 papers in IEEE Journals and Conferences. He chairs the IEEE Working Groups on Insulator Contamination and Dielectric Aging. He was the chair of a committee that prepared IEEE standard (P1523) on High Voltage Insulator Coatings. He is the US representative for CIGRE Study Committee D1 and two working groups dealing with polymeric materials and interfaces in insulating systems. He was elected to IEEE fellow in 1998 for contribution to aging of polymeric materials used for Outdoor HV insulation. He has supervised about 50 graduate students (MS and Ph. D). He teaches a short course on high voltage outdoor insulators that is offered annually at ASU, and at various companies on demand.
	Arthur J. Kroese is a principal engineer at the salt river project (SRP), a public company providing both water and electric power to Central Arizona. The responsibilities of Mr. Kroese include engineering, design and analysis of overhead and underground transmission lines 69, 115, 230 and 500 kV, including preparation of specifications for porcelain and composite insulators at SRP. Mr. Kroese is a registered Professional Engineer in the state of Arizona; a member of IEEE's Power Engineering Society, has been an industry consultant to the Electric Power Research Institute and holds a BSEE from the University of Colorado

LIST OF FIGURES

15 Plot of pixel intensities as a function of distance for different PD magnitudes (the dotted portion of the curves represents the region of extrapolation)

16 Plot of pixel intensity and magnitude under clear and foggy conditions

17 Quantification of corona discharges observed in the field using the proposed method (I)

18 Quantification of corona discharges observed in the field using the proposed method (II)

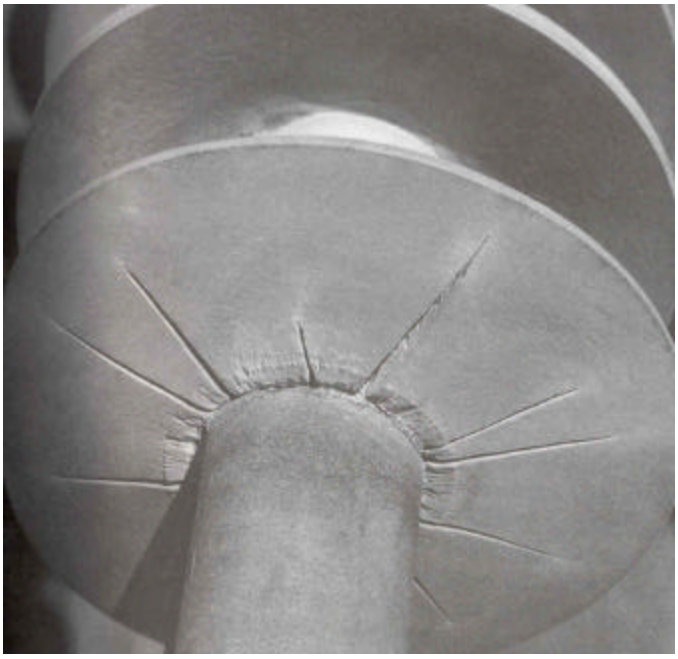

(a)

(b)

Figure 1: Corona cutting of the housing material of two different 230 kV NCI without corona rings in two different stages of degradation. Fig. 1a shows the advanced stage, and Fig. 1b shows degradation in early state.

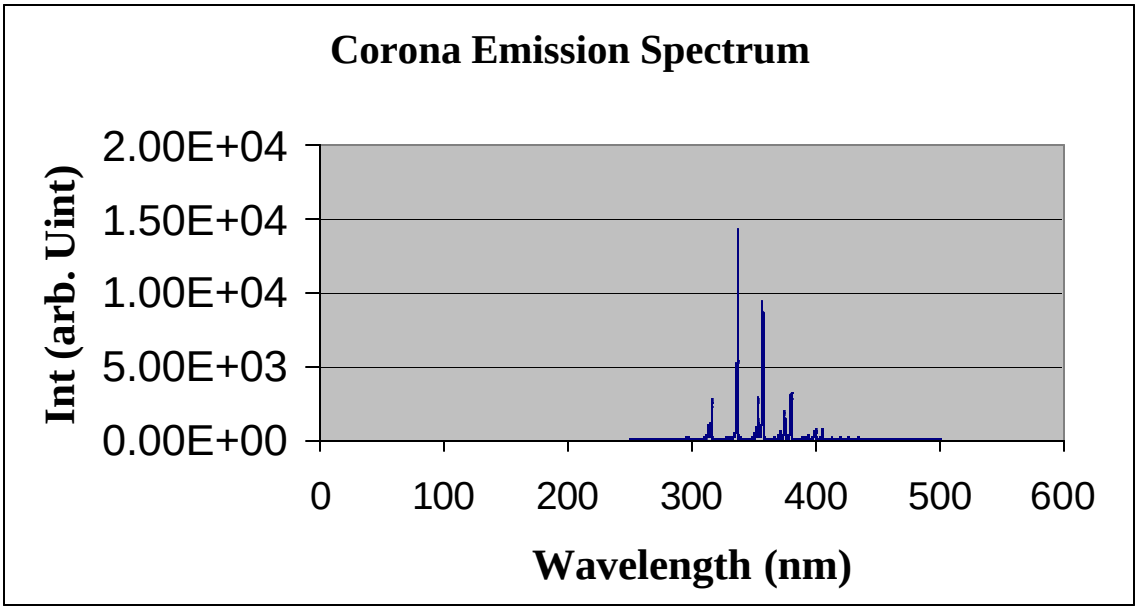

Figure 2: Corona emission spectrum from a point-plane configuration

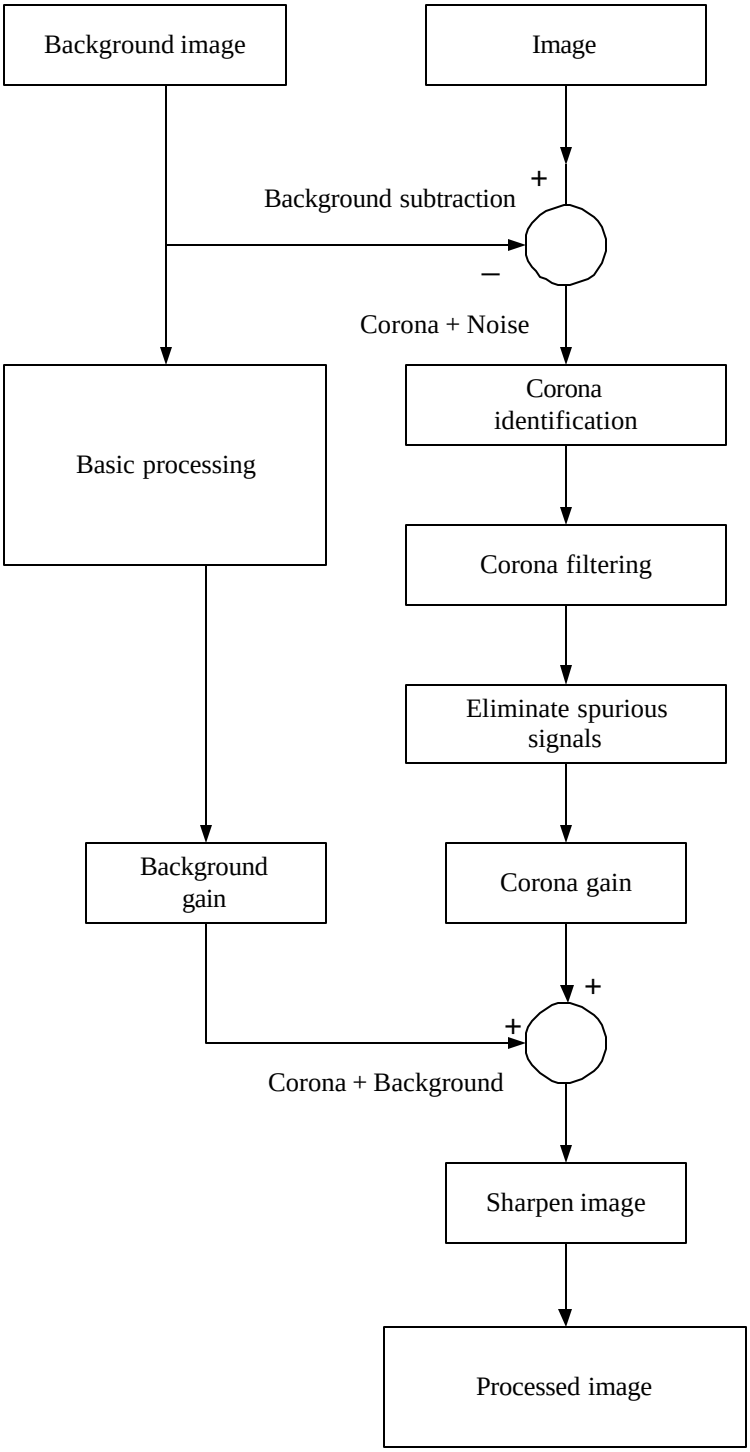

Figure 3: Flow chart for image processing of corona image

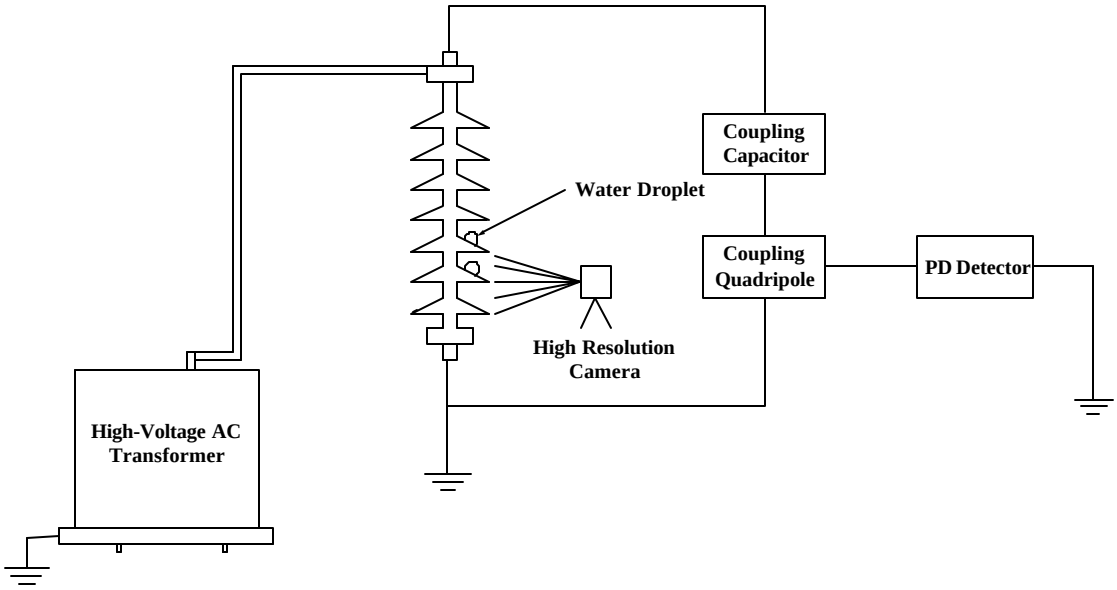

Figure 4: Experimental test Setup

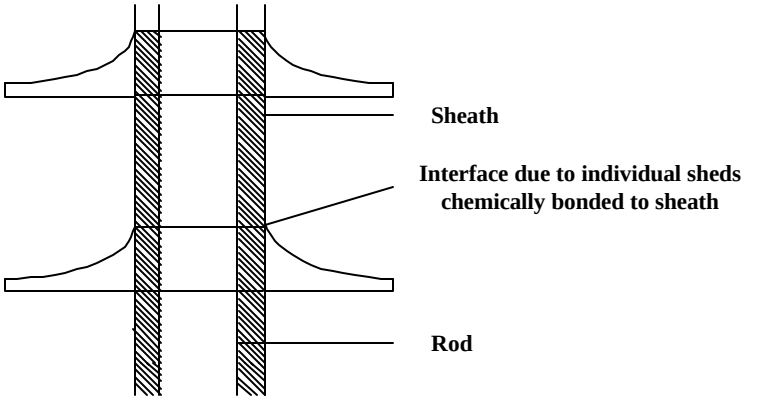

5 (a)

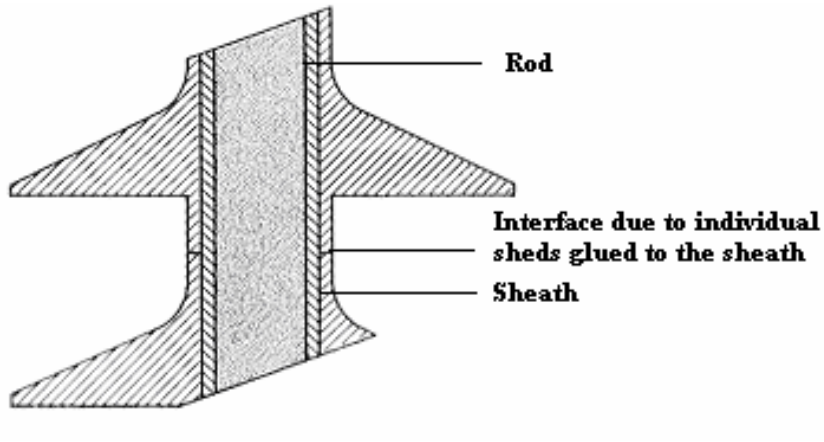

5 (b)

Figure 5: Schematic of the two NCI designs evaluated.

(a)

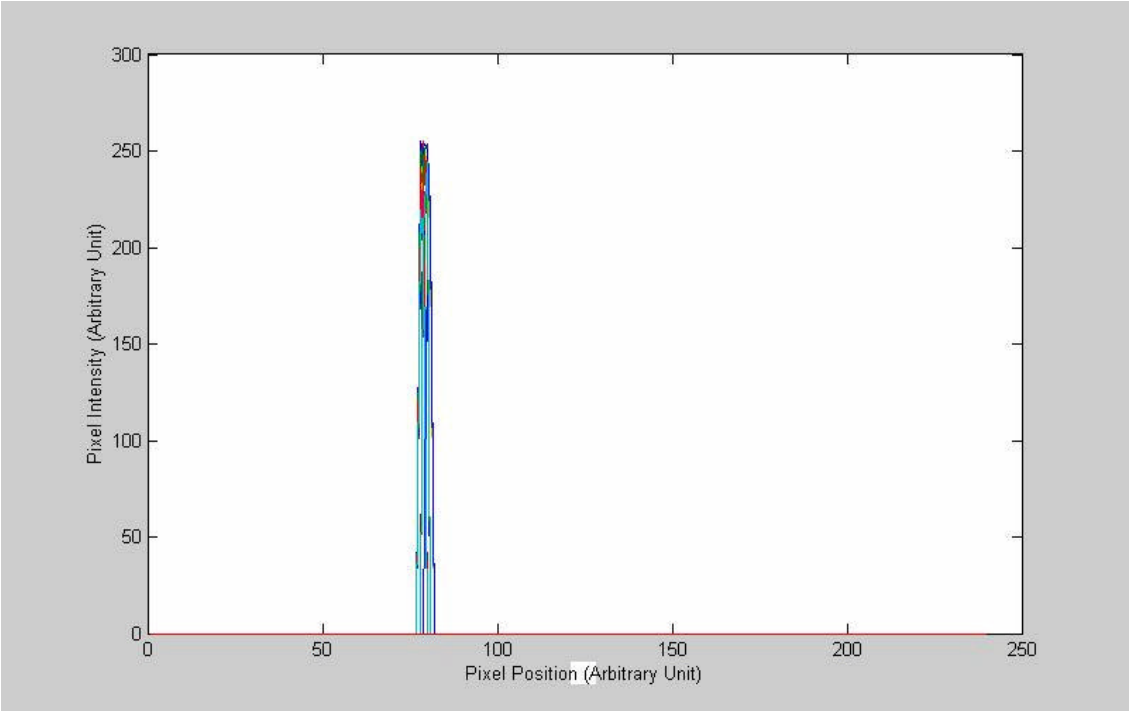

(b)

Figure 6: Corona at 50 kV (0.75 p.u) of magnitude 30 pC from a weathered hardware of a silicone insulator under dry conditions, fig. (a) and corresponding intensity plot fig. (b).

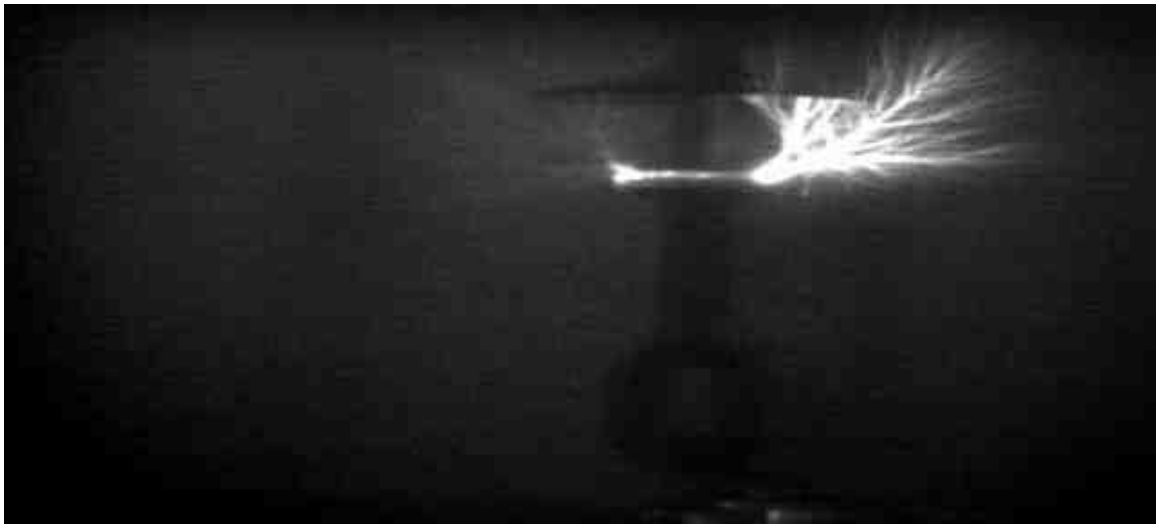

(a)

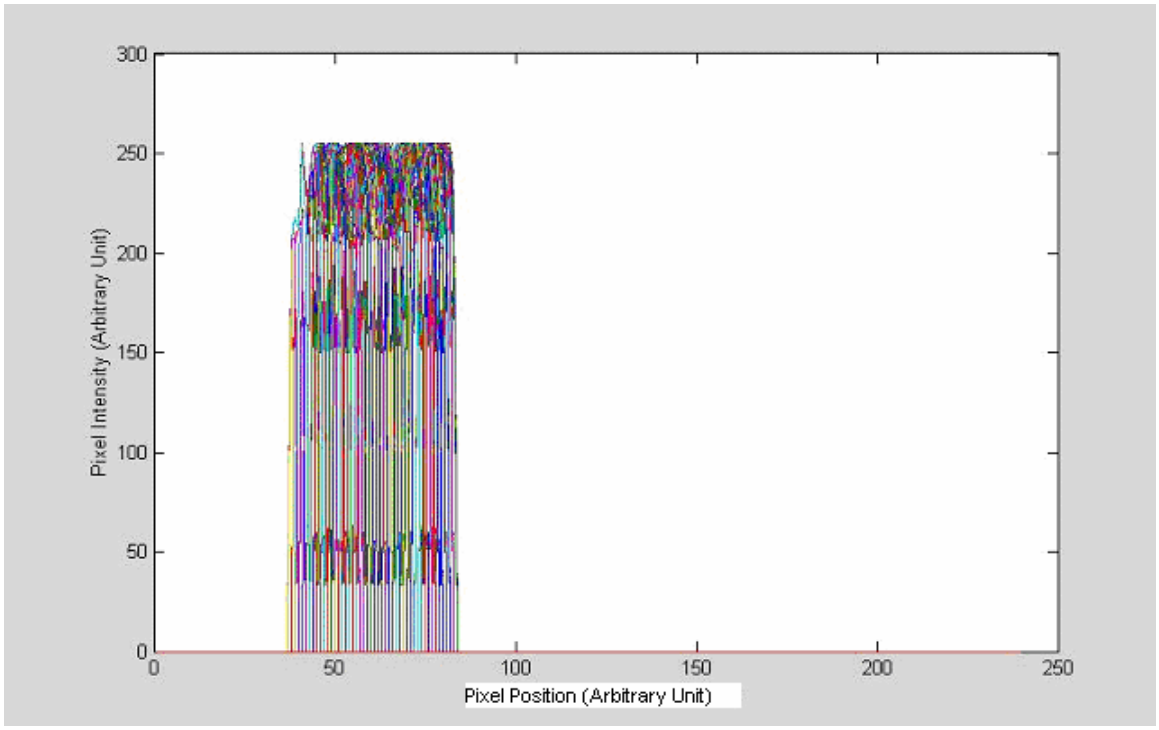

(b)

Figure 7: Corona at 80 kV (1.2 p.u) of magnitude 2.0 nC from a weathered hardware of a silicone insulator under dry conditions, fig. (a) and corresponding intensity plot fig. (b).

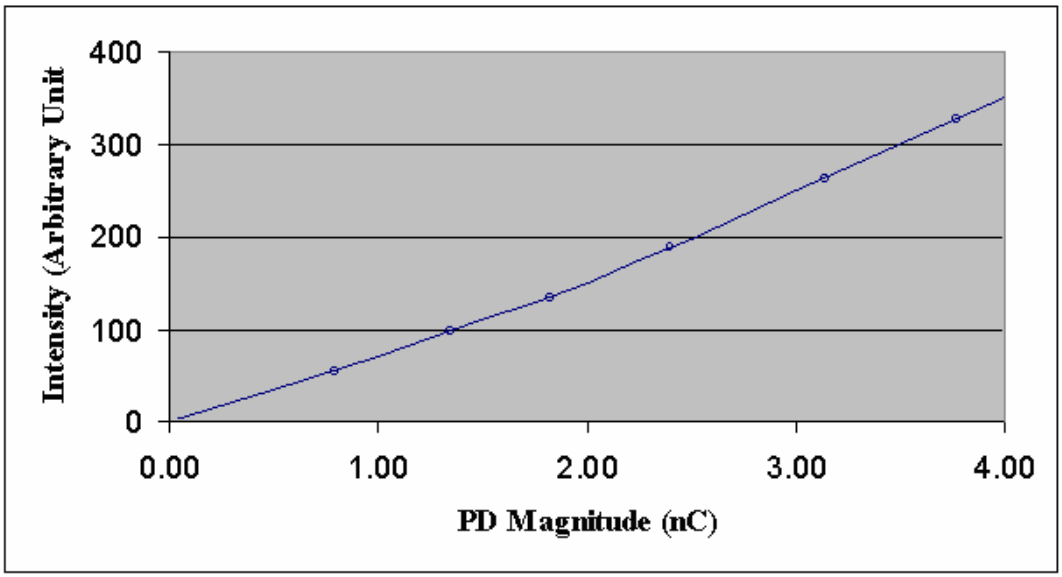

Figure 8: Plot between pixel intensity and PD magnitude

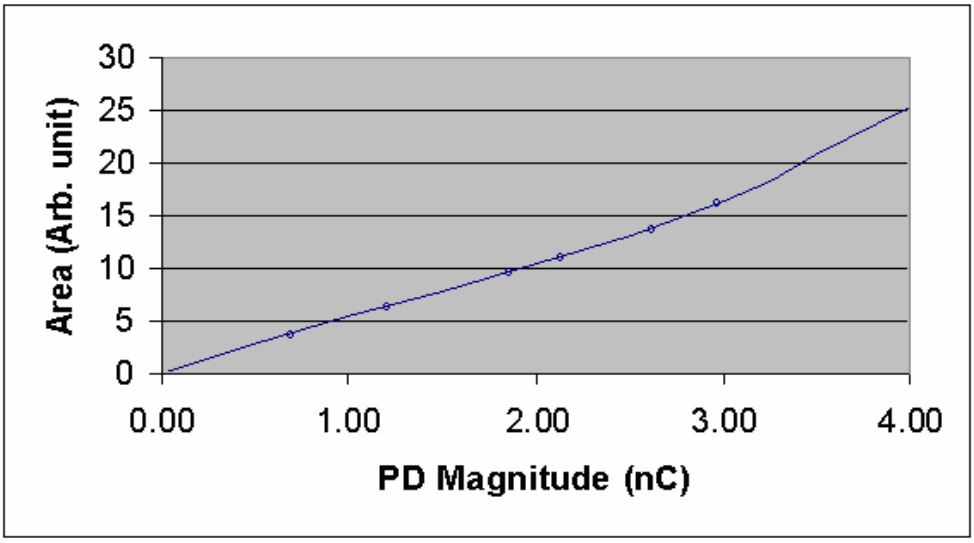

Figure 9: Plot between illuminated pixel area and PD magnitude

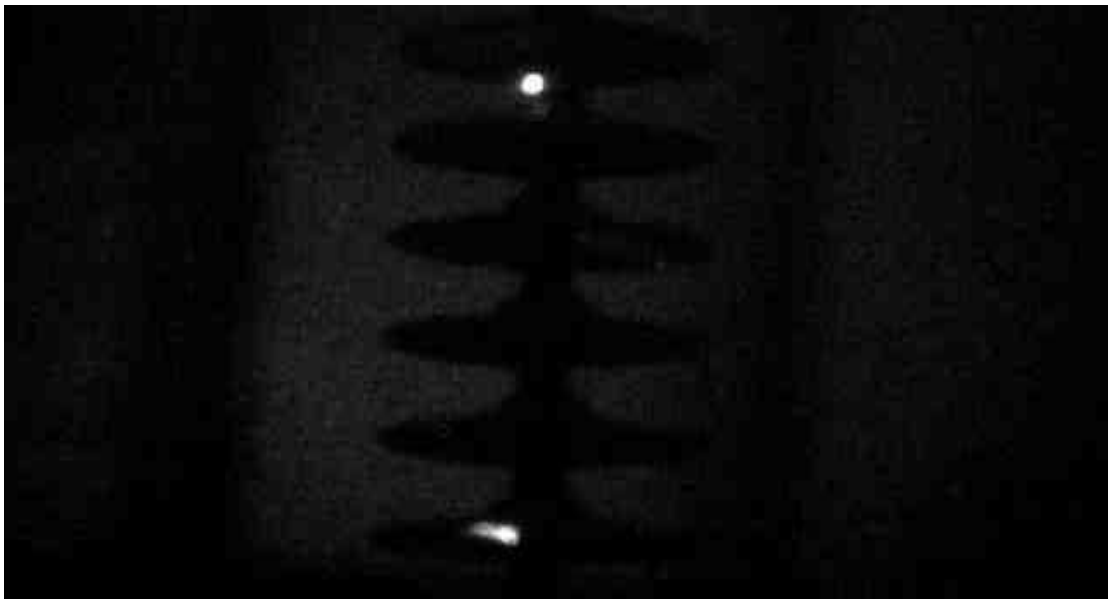

(a)

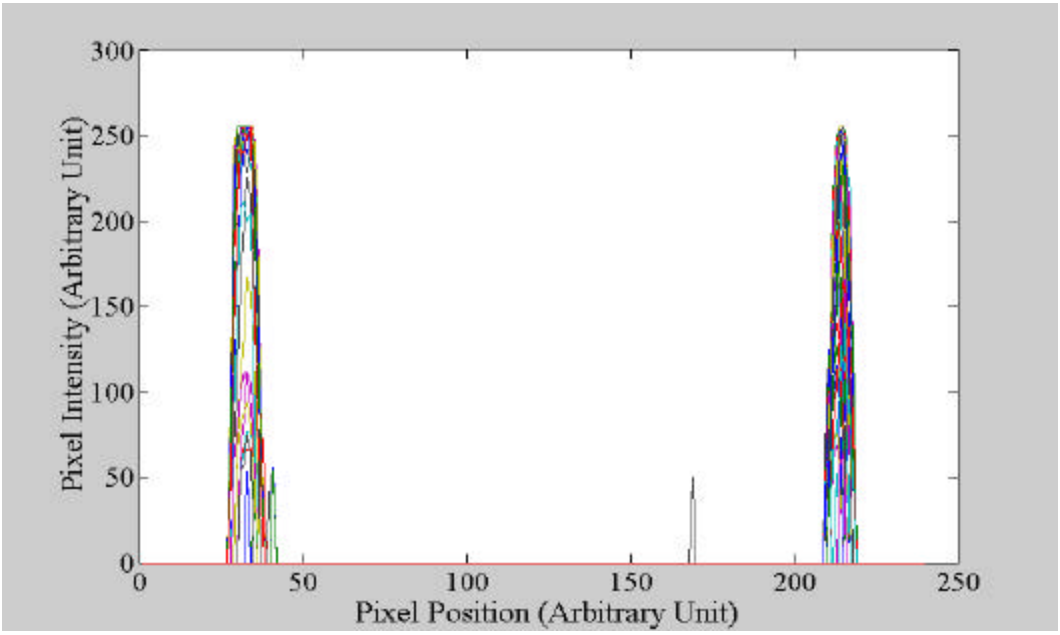

(b)

Figure 10: Discharge of magnitude 0.1 nC on EPDM Insulator at 50 kV (0.75 p.u) under wet condition, fig. (a) and corresponding intensity plot, fig. (b)

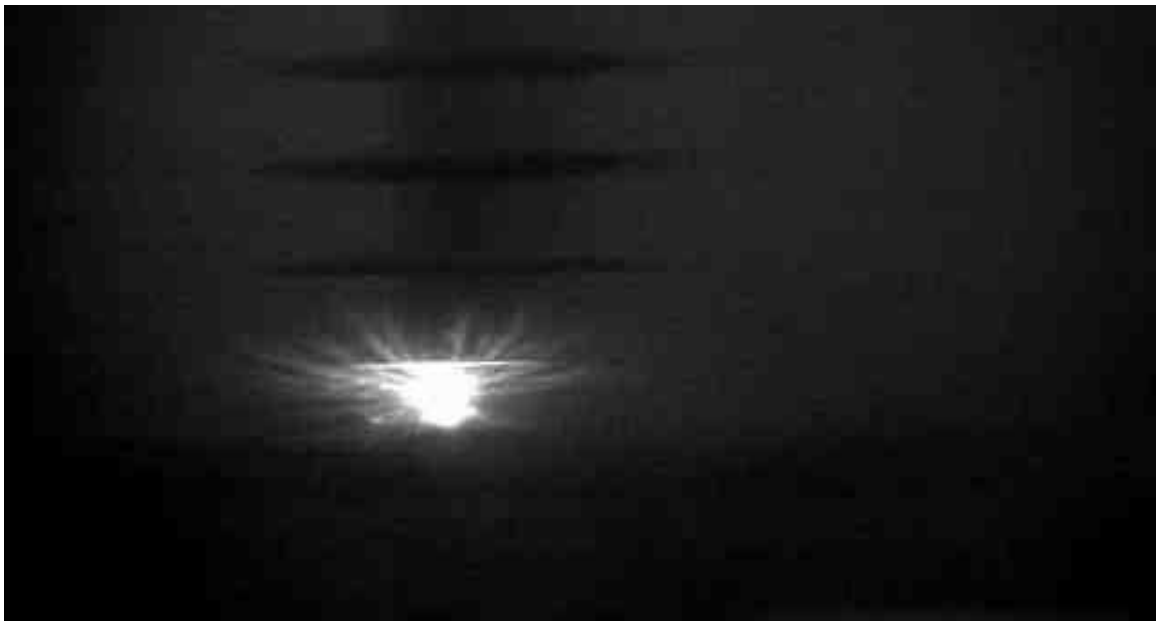

(a)

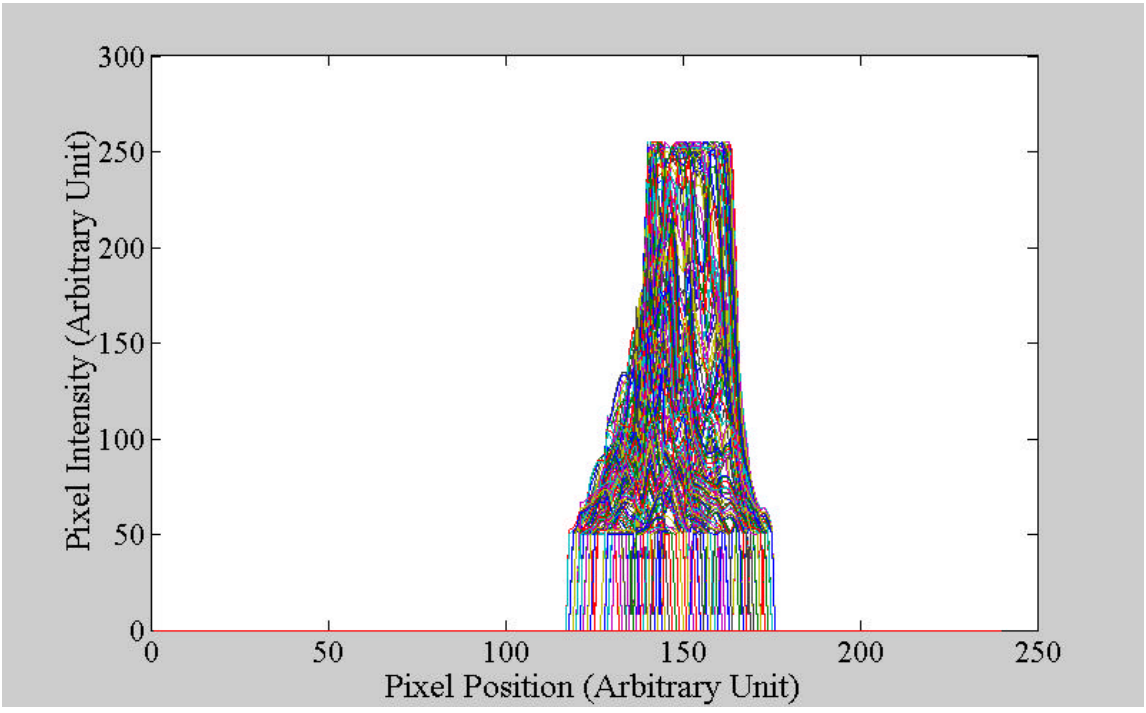

(b)

Figure 11: Discharge on EPDM insulator at 80 KV (1.2 p.u) under wet condition, fig. (a) and corresponding intensity plot, fig. (b)

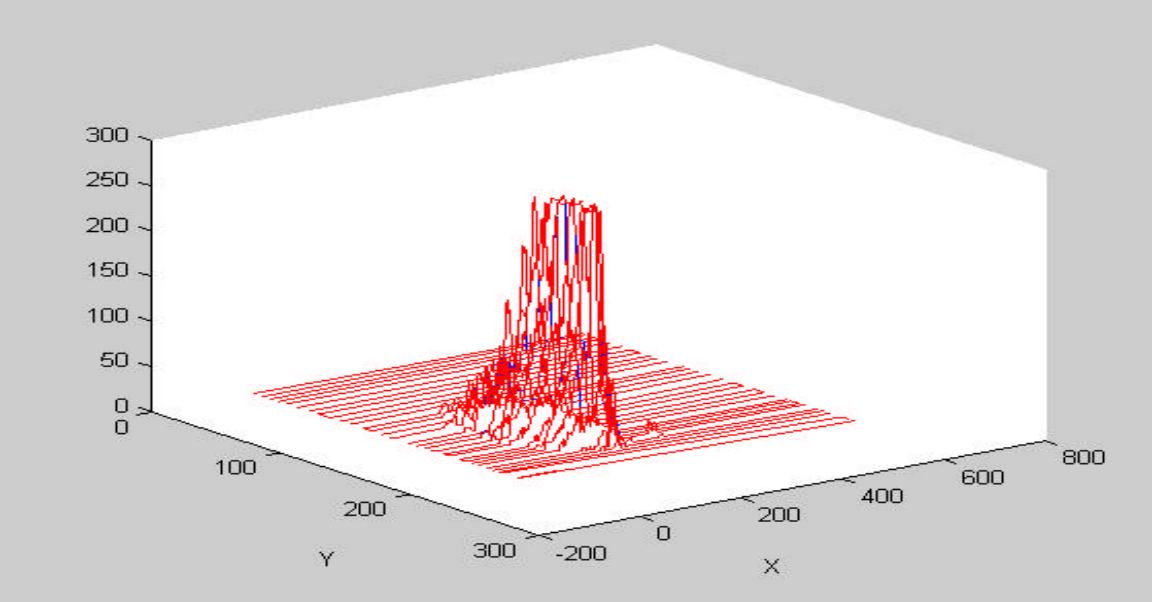

Figure 12: Three-dimensional representation of the intensity distribution for corona in fig. 11 (b)

{X, Y}: Defines the pixel position in the image matrix, Z: Pixel intensity

(a) Corona on hardware at 75 kV (1.1 p.u) under dry conditions

(b) Corona from water drops on the hardware at 30 kV (0.45 p.u)

(c) Corona from water drops on weathershed at 50 kV (0.75 p.u)

(d) Corona from water drops in the interface of shed and shank at 40 kV (0.60 p.u)

(e) Corona in the shank between hardware and the first shed at 60 kV (0.9 p.u) under wet conditions

Figure 13: Typical corona on NCI

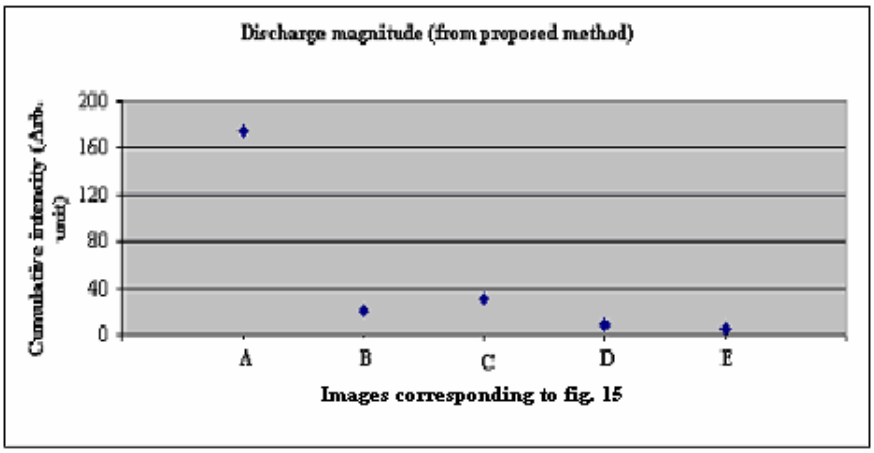

(a)

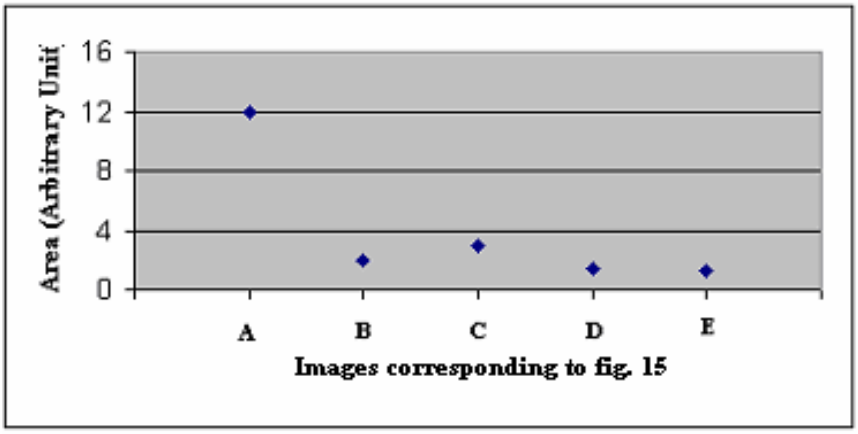

(b)

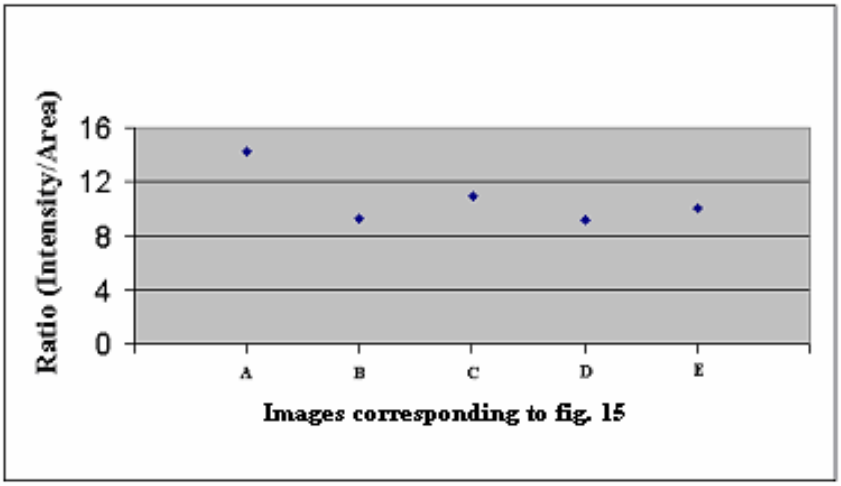

(c)

Figure 14: Cumulative intensity fig. (a), area fig. (b) and normalized intensity-area plot fig. (c) corresponding to images in fig. 13 by using the proposed method

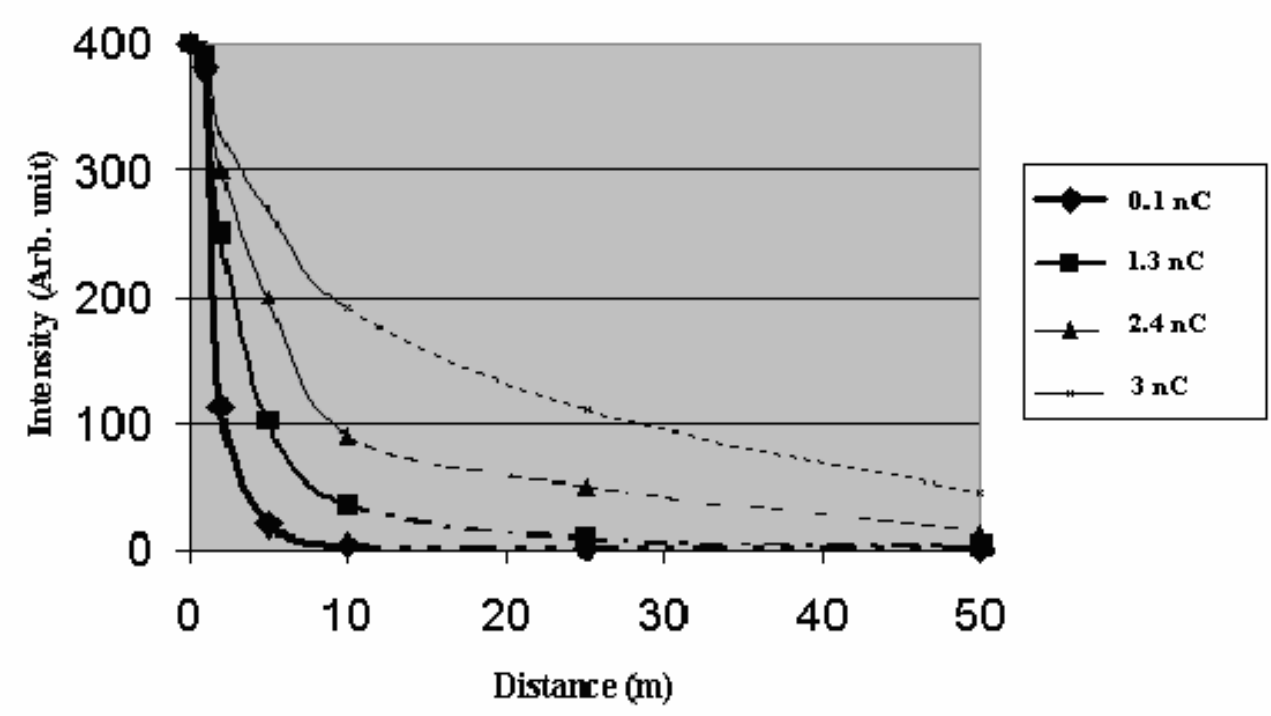

Figure 15: Plot of pixel intensities as a function of distance for different PD magnitudes (the dotted portion of the curves represents the region of extrapolation)

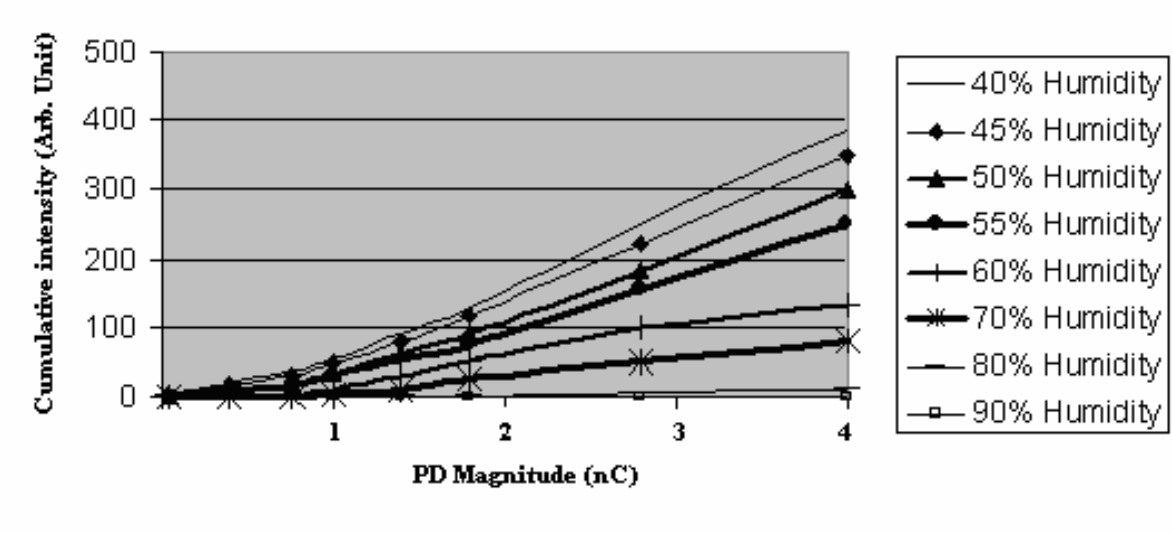

Figure 16: Plot of pixel intensity and magnitude under clear and foggy conditions (With a distance of 5 m between the camera and the point of interest)

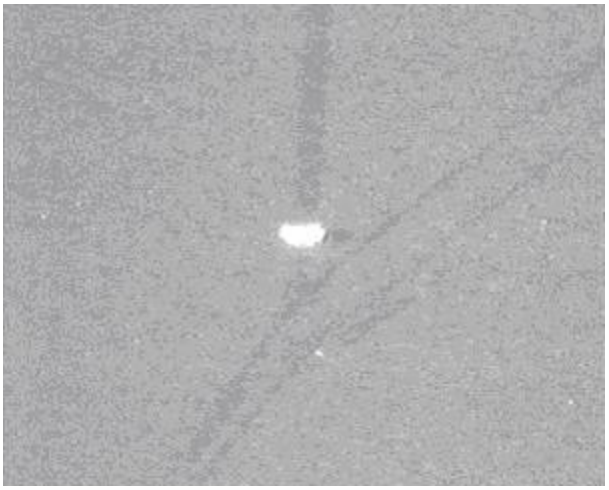

(a) Corona originating at the metal fittings of a 230 kV suspension NCI operating in a desert environment

(b) Processed corona image corresponding to Fig. 17 (a)

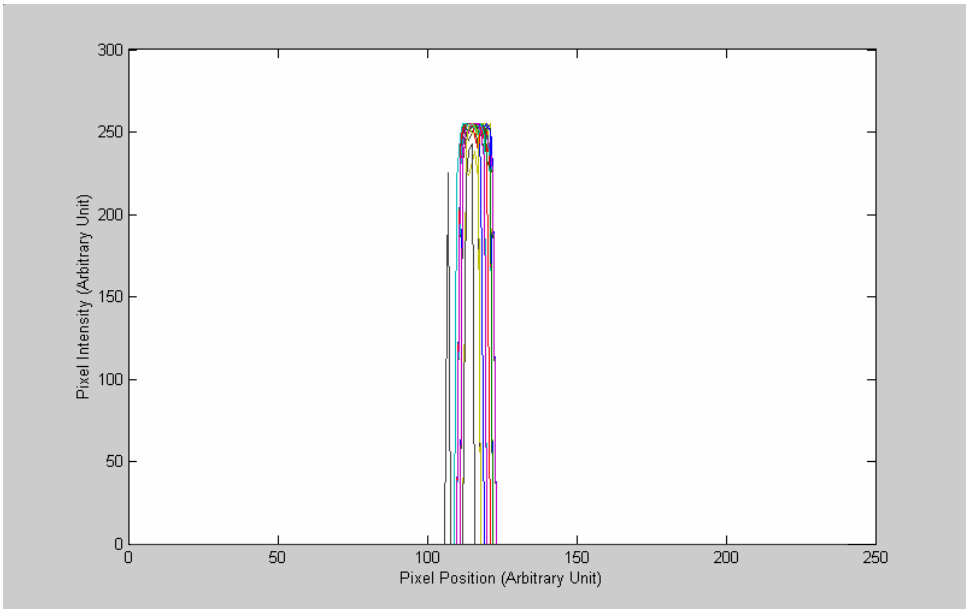

(c) Intensity Plot corresponding to corona seen in Fig. 17 (b)

Figure 17: Quantification of corona discharges observed in the field using the proposed method

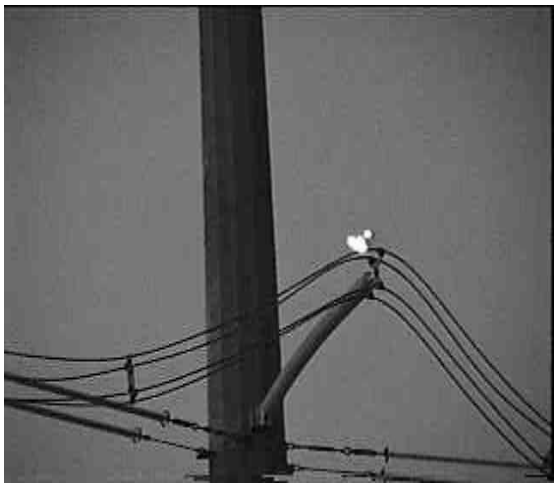

(a) Corona originating at the metal fittings of a 500 kV jumper line post NCI operating in a desert environment

(b) Processed corona image corresponding to Fig. 18 (a)

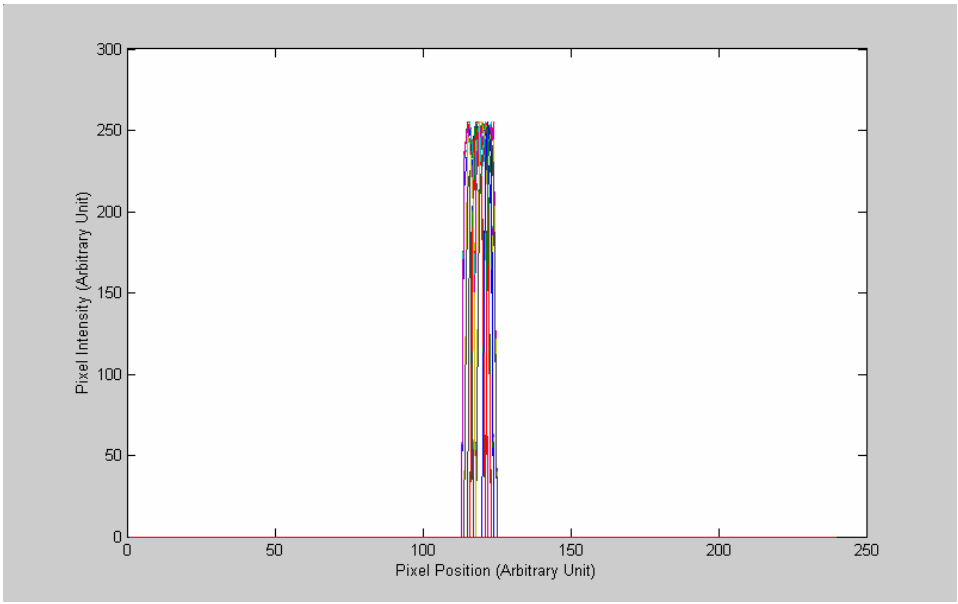

(c) Intensity Plot corresponding to corona seen in Fig. 18 (b)

Figure 18: Quantification of corona discharges observed in the field using the proposed method